Spin correlations in the pyrochlore slab compounds $Ba_2Sn_2Ga_{10-7p}ZnCr_{7p}O_{22}$

2004 J. Phys.: Condens. Matter 16 S835

(http://iopscience.iop.org/0953-8984/16/11/038)

INSTITUTE OF PHYSICS PUBLISHING JOURNAL OF PHYSICS: CONDENSED MATTER

J. Phys.: Condens. Matter **16** (2004) S835–S842 PII: S0953-8984(04)74129-6

Spin correlations in the pyrochlore slab compounds $Ba_2Sn_2Ga_{10-7p}ZnCr_{7p}O_{22}$*

P Bonnet[1], C Payen[1,4], H Mutka[2], M Danot[1], P Fabritchnyi[1], J R Stewart[2], A Mellergård[3] and C Ritter[2]

[1] Institut des Matériaux Jean Rouxel, UMR6502 CNRS—Université de Nantes, BP32229, 44322 Nantes Cedex 3, France
[2] Institut Laue Langevin, Grenoble, France
[3] Studsvik Neutron Research Laboratory, Nykoping, Sweden

E-mail: christophe.payen@cnrs-imn.fr

Received 7 January 2004
Published 4 March 2004
Online at stacks.iop.org/JPhysCM/16/S835 (DOI: 10.1088/0953-8984/16/11/038)

Abstract

The low-temperature properties of a diluted antiferromagnetic pyrochlore slab of $S = 3/2$ spins are investigated through a study of the frustrated oxides $Ba_2Sn_2Ga_{10-7p}ZnCr_{7p}O_{22}$ ($p > 0.85$). Powder neutron diffraction and ^{119}Sn Mössbauer absorption show no evidence of long-range magnetic order above 1.5 K. As in $SrCr_{9q}Ga_{12-9q}O_{19}$, diffuse magnetic scattering, indicative of short range spin–spin correlations, is observed at low temperature. The dependence of the low-temperature sub-Curie bulk susceptibility to weak site depletion is the inverse of that observed in $SrCr_{9q}Ga_{12-9q}O_{19}$.

(Some figures in this article are in colour only in the electronic version)

1. Introduction

One of the main motivations of the current interest shown in frustrated magnets is the suggestion that geometric frustration might lead to macroscopic degeneracies and cooperative ground states with dynamic or quasi-static short range magnetic order [1]. In this context, insulating transition metal oxides with atomic spins on the vertices of corner-sharing triangles or tetrahedra provide the opportunity to check theoretical results obtained for ideal frustrated lattices such as the pyrochlore or Kagomé antiferromagnetic networks [1]. The recent discovery of the new chromium oxides $Ba_2Sn_2Ga_{10-7p}ZnCr_{7p}O_{22}$ (BSGZCO), for instance, has brought up the possibility of extending the studies concerning the effects of quenched structural disorder in an antiferromagnetic pyrochlore slab of $S = 3/2$ spins [2]. These compounds,

* Dedicated to the memory of Pierre Colombet (1950–2003).
[4] Author to whom any correspondence should be addressed.

which have a more two-dimensional magnetic lattice than the well-known pyrochlore slab compound $SrCr_{9q}Ga_{12-9q}O_{19}$ (SCGO) [3], have been recently characterized by powder neutron diffraction at room temperature, bulk susceptibility and specific heat measurements [2]. Like in SCGO, the crystal structure of BSGZCO features magnetic slabs with two identical Kagomé layers enclosing a triangular plane, so pyrochlore slabs made of corner-sharing tetrahedra of Cr^{3+} ($S = 3/2$) ions are formed. In both BSGZCO and SCGO, random dilution of the pyrochlore slabs is realized by substituting nonmagnetic Ga^{3+} ions for the Cr^{3+} ions. Bulk susceptibility and specific heat data for BSGZCO ($p > 0.85$) show typical signatures of geometric frustration. In particular, the Curie–Weiss behaviour of the susceptibility extends to temperatures smaller than what could be expected from the Weiss temperature. Also, a spin-glass-like transition is observed near $T_f = 1.5$ K.

In this paper, we present a study of the spin correlations in BSGZCO for $p = 0.97$ and 0.86. Powder samples were examined by bulk magnetization, neutron diffraction and ^{119}Sn Mössbauer spectroscopy. Our observations confirm and complete those done earlier by Hagemann *et al* [2]. Our data show no evidence of magnetic long-range order above 1.5 K. Diffuse magnetic scattering is observed at low temperature. Below 4 K, ^{119}Sn Mössbauer spectra exhibit a magnetic contribution with a distribution of hyperfine fields. The low-temperature susceptibility decreases as the site dilution increases, in contrast to the behaviour observed for SCGO. This suggests qualitative differences in the behaviour of these pyrochlore slab systems.

2. Experimental details

Powder samples with $p = 0.97$ and 0.86 were prepared through conventional solid-state reactions in air [2] and first characterized by energy-dispersive x-ray analysis. The results of these analyses are consistent with the nominal compositions. Ac susceptibility and dc magnetization data were obtained down to 2 K using a commercial SQUID magnetometer. These data were corrected for the ionic diamagnetic contributions. Ac susceptibility data show no sign of a magnetic transition above 2 K. Mössbauer spectra were recorded on a thin sample down to 1.6 K. High-resolution neutron powder diffraction data were collected at $T = 290$, 50 and 1.5 K on the D2B diffractometer at the ILL (incoming wavelength $\lambda = 0.159\,43$ nm) using 5 g samples. Diffraction experiments with neutron polarization analysis [4] were performed on the D7 instrument at the ILL (incoming wavelength $\lambda = 0.48$ nm).

3. Results and discussion

The neutron diffraction patterns were analysed by means of the Rietveld method, using the FULLPROF program [5] with a pseudo-Voigt profile function. Figure 1 shows the diffraction data collected at 290 K for $p = 0.97$. The starting model for the crystal structure was adopted from the results in [2]. Structure refinement parameters for the room temperature data are shown in table 1. These parameters are consistent with the study in [2]. Within the pyrochlore slab, the values of the Cr–Cr distances and the Cr–O–Cr angles are very close to those observed in SCGO. A magnetostructural analysis, following that of [6] leads to the existence of two antiferromagnetic (AF) exchange constants which have the same order of magnitude. In SCGO, the average AF coupling is $J_{slab} \approx 80$ K [6].

The reciprocal dc susceptibility data, shown in figure 2, compare well with previous data reported in [2]. Curie–Weiss fits done to the high temperature susceptibility are consistent with $S = 3/2$ Cr^{3+} ions; the effective moments per Cr^{3+} are in the range 3.75–3.80 μ_B, versus

Table 1. Structure refinement parameters for $Ba_2Sn_2Ga_{10-7p}ZnCr_{7p}O_{22}$, $p = 0.97$ (first line) and $p = 0.86$ (second line), at 290 K in the space group $P\bar{3}m1$ (no 164). Parameters reported without errors (indicated in parenthesis) were fixed in the refinement. Cell parameters: $a = b = 0.585\,68(1)$ nm; $c = 1.42\,537(3)$ nm; $a = b = 0.585\,73(2)$ nm; $c = 1.425\,49(5)$ nm; reliability factors (%): $R_p = 4.15$, $R_{wp} = 5.38$; $R_p = 3.35$, $R_{wp} = 4.21$.

Atom (Wyckoff site)	x	y	z	B (Å^2)	Fractional occupancy
Ba(2d)	1/3	2/3	0.4253(5)	1.1(1)	1.00
	1/3	2/3	0.4248(4)	1.05(8)	1.00
Sn(2d)	1/3	2/3	0.6815(4)	0.49(9)	1.00
	1/3	2/3	0.6809(3)	0.43(5)	1.00
Zn(2d)	1/3	2/3	0.9556(3)	0.72(7)	0.50
	1/3	2/3	0.9557(3)	0.68(6)	0.50
Ga(2d)	1/3	2/3	0.9556(3)	0.72(7)	0.50
	1/3	2/3	0.9557(3)	0.68(6)	0.50
Ga(2c)	0	0	0.3734(3)	0.66(8)	1.00
	0	0	0.3735(2)	0.55(6)	1.00
Cr(1a)	0	0	0	1.0(2)	0.97
	0	0	0	0.2(2)	0.86(2)
Ga(1a)	0	0	0	1.0(2)	0.03
	0	0	0	0.2(2)	0.14(2)
Cr(6i)	0.1691(6)	−0.1691(6)	0.1695(2)	0.50(8)	0.97
	0.1684(4)	0.1684(4)	0.1701(2)	0.5	0.87(1)
Ga(6i)	0.1691(6)	−0.1691(6)	0.1695(2)	0.50(8)	0.03
	0.1684(4)	0.1684(4)	0.1701(2)	0.5	0.13(1)
O1(2c)	0	0	0.2399(4)	0.20(9)	1.00
	0	0	0.2396(3)	0.29(7)	1.00
O2(2d)	1/3	2/3	0.0913(4)	0.2(1)	1.00
	1/3	2/3	0.0917(3)	0.35(8)	1.00
O3(6i)	0.1551(4)	−0.1551(4)	0.9141(3)	0.90(7)	1.00
	0.1542(3)	−0.1542(3)	0.9138(2)	0.85(5)	1.00
O4(6i)	0.4926(4)	−0.4926(4)	0.2440(2)	0.93(5)	1.00
	0.4929(3)	−0.4929(3)	0.2427(2)	0.78(4)	1.00
O5(6i)	0.1742(4)	−0.1742(4)	0.5938(2)	0.87(6)	1.00
	0.1739(3)	−0.1739(3)	0.5935(1)	0.94(4)	1.00

an expectation of 3.83 μ_B, assuming $g = 1.98$ (this value was obtained for SCGO [7]). The results of Mondelli *et al* [8] obtained for powder samples of SCGO are also shown in figure 2. The susceptibility per chromium is significantly lower in SCGO than in BSGZCO since the susceptibility of Cr–Cr isolated spin pairs with a strong AF coupling of $J \approx 220$ K also contributes to the macroscopic susceptibility of SCGO [6, 8]. Above $T = 150$ K, all samples exhibit susceptibility behaviour consistent with geometric frustration, since the mean-field Curie–Weiss regime extends to temperatures much lower than what could be expected from the Weiss temperature ($\theta_W \approx -365$ and -315 K for $p = 0.97$ and 0.86, respectively). The puzzling behaviour of the low-temperature susceptibility will be discussed hereafter. The results in [2] indicate a spin-glass-like transition near 1.5 K for BSGZCO, while the powder samples of SCGO exhibit a spin-glass behaviour below $T_f = 3.4$ and 3.2 K for $q = 0.98$ and 0.89, respectively (figure 2) [8]. The behaviour of the nonlinear magnetization has also been analysed by writing the magnetization $M(H, T)$ as an expansion in odd powers of the applied field H:$M(H, T) = \chi_1 H - a_3(\chi_1 H)^3 + a_5(\chi_1 H)^5 - \cdots$. In this expression, χ_1 is the linear susceptibility and the coefficients a_{2n+1} are functions of temperature (the nonlinear

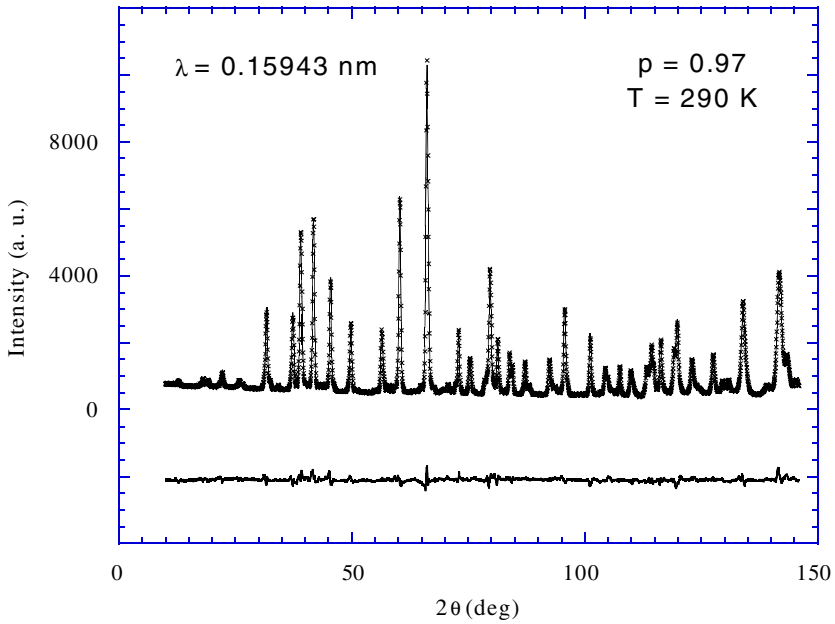

Figure 1. Computed (solid curves) and observed (crosses) powder neutron diffraction data for $Ba_2Sn_2Ga_{10-7p}ZnCr_{7p}O_{22}$ ($p = 0.97$) at $T = 290$ K. The lower curve shows the difference between the observed and computed data on the same scale.

terms $a_{2n+1}(T)$ are expected to show power-law divergences upon approaching a critical spin-glass temperature T_g) [9]. For $p = 0.97$, the $a_3(T)$ coefficient has a power-law divergence, $a_3 \propto (T/T_f - 1)^{-\gamma}$ with $\gamma \approx 2$ and $T_f = 1.2(1)$ K, in the temperature range 2–4 K, and for $\mu_0 H < 0.2$ T.

^{119}Sn Mössbauer spectroscopy measurements were performed in the 300–1.6 K range. Above 4 K, the spectra exhibit a unique unresolved quadrupole doublet ($\Delta = 0.24$ mm s^{-1} at 300 K) with isomer shift values ($\delta = 0.04$ mm s^{-1} versus $CaSnO_3$, at 300 K) indicative of Sn(IV) species in an octahedral environment. This is fully consistent with the crystal structure proposed in [2]. Below 4 K, an unresolved magnetic contribution spreading over a narrow velocity range is observed. This magnetic contribution can be described by a distribution of hyperfine fields in the 10–60 kG range at the ^{119}Sn sites for $T = 1.6$ K (figure 3). The weakness of the transferred fields is consistent with both the crystal structure and the $t_{2g}^3 e_g^0$ electronic structure of the Cr^{3+} ions. The main superexchange interactions responsible for the spin polarization transfer to the diamagnetic Mössbauer element concerns the t_{2g} orbital of Cr^{3+}, and this transfer is weak because the t_{2g} and oxygen 2p orbitals do not overlap in a favourable way (130° pathways).

The absence of static long-range order is confirmed by high-resolution neutron powder diffraction data which show no evidence of magnetic Bragg peaks above 1.5 K. However, diffuse scattering with a form similar to that observed in SCGO [10] is present over a notable Q range, centred at about 15 nm^{-1} (figure 4). These correlations, visible in the D2B data that also contain nuclear scattering contributions, are magnetic in nature, as shown using neutron polarization analysis on the D7 instrument to separate the magnetic from the nuclear scattering (figure 4). Therefore the diffuse scattering indicates the presence of short-range antiferromagnetic correlations. The fact that the magnetic scattering in figure 4 appears to

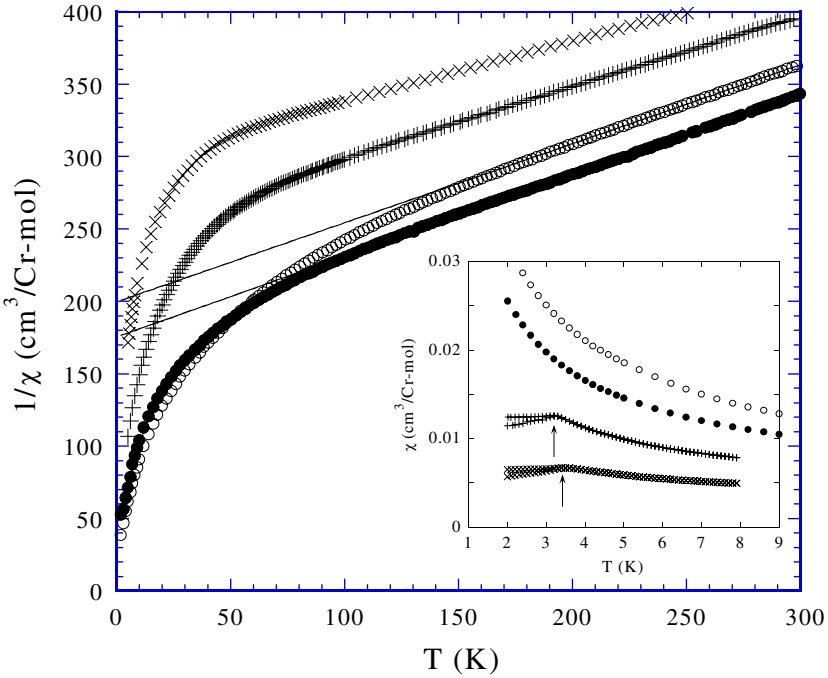

Figure 2. The temperature-dependent inverse magnetic susceptibility (obtained at $H = 1$ kOe) of $Ba_2Sn_2Ga_{10-7p}ZnCr_{7p}O_{22}$ for $p = 0.97$ (open circles) and $p = 0.86$ (solid circles). Solid lines represent Curie–Weiss fits done for $T > 200$ K. For comparison, previous data reported in [8] and obtained for powder samples of $SrCr_{9q}Ga_{12-9q}O_{19}$ with $q = 0.98$ (crosses) and $q = 0.89$ (plus signs) are displayed. Inset: a plot of the low-temperature susceptibility (obtained at $H = 10$ Oe) for the same samples (same symbols as in the main figure). Zero-field-cooled and field-cooled susceptibilities are shown for the $SrCr_{9q}Ga_{12-9q}O_{19}$ samples. Arrows indicate the freezing temperatures.

vanish as Q goes to zero suggests that the low temperature state consists of nanoscale spin clusters carrying no net magnetization [11]. A preliminary inelastic neutron scattering study revealed the dynamic nature of this diffuse scattering [12], showing that it extends up to 35 meV.

We turn now to the behaviour of the bulk susceptibility $\chi(T)$ at low-temperature, above the spin-glass-like transition. In this regime, the high-temperature Curie–Weiss law is no longer obeyed (figure 2). The susceptibility keeps on rising down to 2 K, but this behaviour is still consistent with antiferromagnetism since the χT product decreases as the temperature decreases. As shown in figure 2, the low-temperature susceptibility per chromium is higher in the $p = 0.97$ compound than in the $p = 0.86$ variant, in contrast with the dilution enhanced susceptibility observed for SCGO [6, 8]. This observation is difficult to reconcile with the usual description applied to SCGO, according to which the low-temperature susceptibility essentially originates from dilution-induced effective spins [6]. This surprising behaviour could originate from the crystal structure. Indeed, an additional type of quenched structural disorder should be present in BSGZCO. Unlike in SCGO, each pyrochlore slab contains oxygen tetrahedra which are equally occupied by Ga^{3+} or Zn^{2+} ions in a random manner, regardless of dilution [2]. Differences in valences and ionic radius for these two nonmagnetic ions should yield lattice strains that in turn should lead to local changes in spin Hamiltonian. For instance, bond disorder could exist in the material. A comparable situation is the case of the isovalent

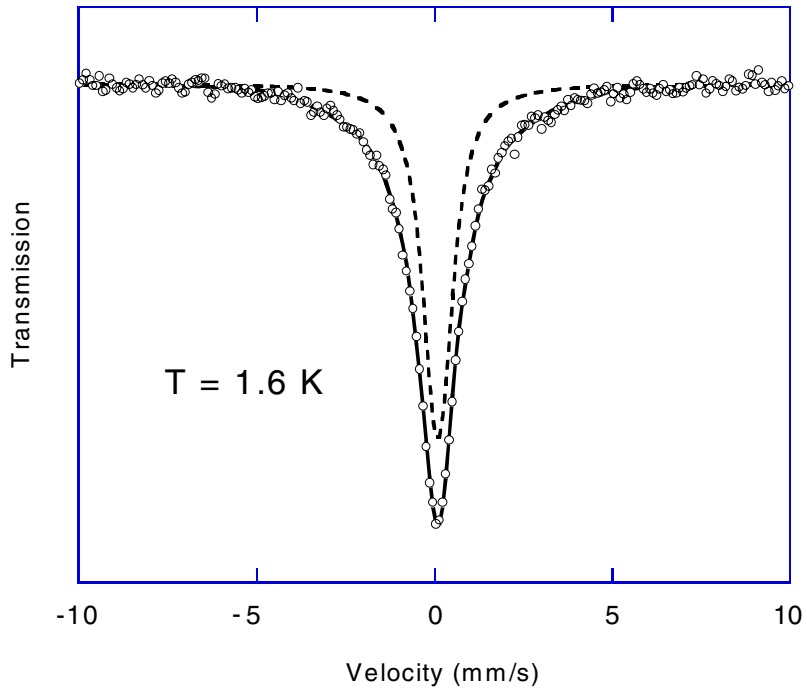

Figure 3. The ^{119}Sn Mossbauer spectrum (open circles) of $Ba_2Sn_2Ga_{10-7p}ZnCr_{7p}O_{22}$ ($p = 0.97$) at $T = 1.6$ K. This spectrum is reproduced (solid curve) considering the coexistence of nonmagnetic (dotted curve) and magnetic (10 kG $< H <$ 60 kG) contributions.

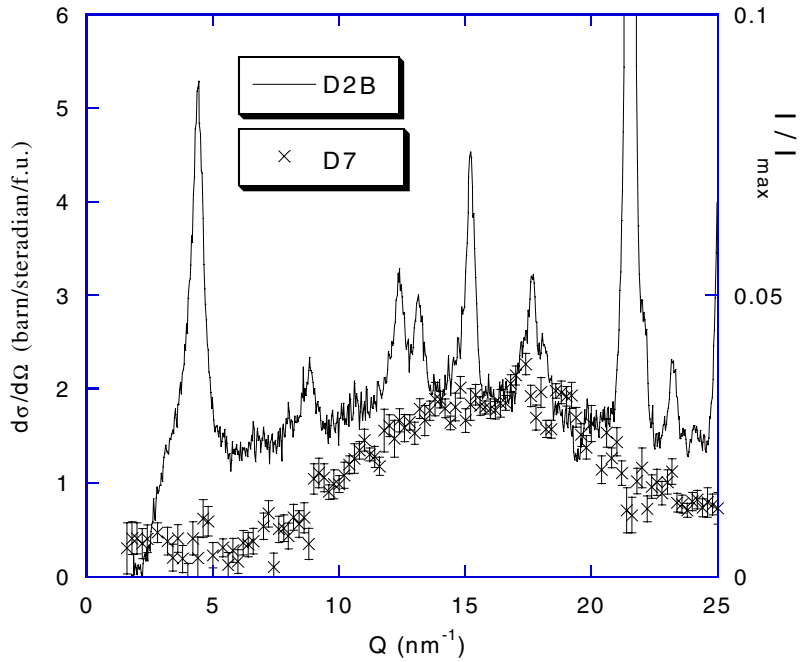

Figure 4. The diffuse scattering observed in the low-Q region on the D2B and D7 two-axis instruments (ILL) at $T = 1.5$ K. The absolute differential magnetic cross section ($d\sigma/d\Omega$) extracted from the (D7) polarized neutron data is in units of b sr^{-1} fu^{-1}. The conventional (D2B) diffraction intensities are normalized to the intensity maximum.

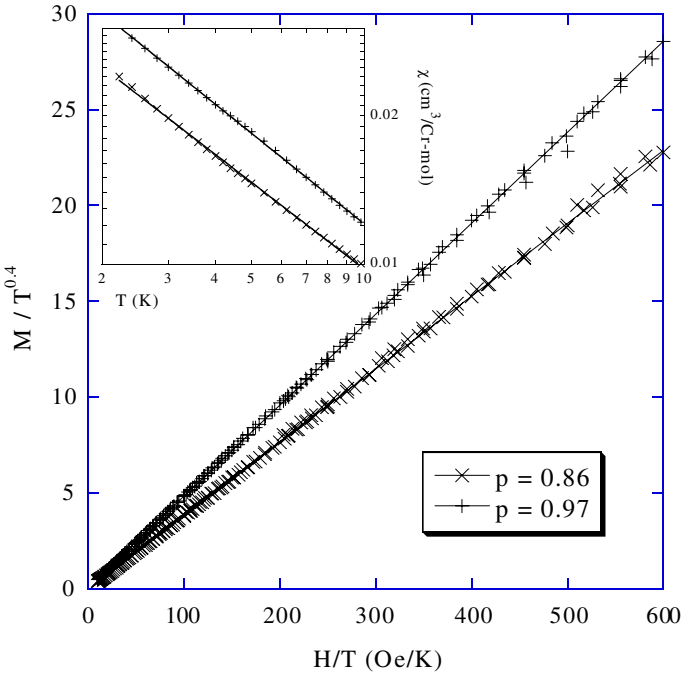

Figure 5. The linear variation of $M(H,T)/T^{1-\alpha}$ with H/T for $Ba_2Sn_2Ga_{10-7p}ZnCr_{7p}O_{22}$ ($\alpha = 0.6$). Straight lines are guides for the eyes. Data obtained in the 2–10 K range have been used for this plot. Inset: a log–log plot of the low-temperature susceptibility (obtained at $H = 100$ Oe) for the same samples. Straight lines represent power-law behaviours, $\chi \propto T^{-\alpha}(\alpha \approx 0.6)$.

substitution of Cd^{2+} for Zn^{2+} in the spinel compound $ZnCr_2O_4$, which leads to a significant increase of low-temperature susceptibility [13] in this compound.

To gain more insight into the susceptibility behaviour, we first tried to analyse the data with the two-population model proposed by Schiffer and Daruka [14], $\chi(T) = \frac{C}{T-\theta_W} + \frac{C_{def}}{T-\theta_{def}}$. In this expression, the first term takes into account the contribution of correlated spin clusters and the second term is related to paramagnetic defects originating from dilution or bond disorder. This two-component expression reproduces well the $\chi(T)$ data in figure 2 using the following parameters: $C \approx 1.8(1.8)$ cm^3 K Cr mol^{-1}, $\theta_W \approx -425$ (-365) K, $C_{def} \approx 0.083$ (0.056) cm^3 K Cr mol^{-1}, $\theta_{def} \approx -1.8$ (-1.2) K and for $p = 0.97$ (0.86). The C_{def}/C ratio is 4.6 (3.1) % for $p = 0.97$ (0.86). Alternately, the low-temperature susceptibility of BSGZCO can be described by a sub-Curie power-law form, $\chi = M/H \propto T^{-\alpha}$ with $\alpha \approx 0.6$ (figure 5). All magnetization data $M(H,T)$ exhibit, in fact, a power-law behaviour in the linear regime of the isothermal response $M(H)$ for $T < 10$ K. This can be seen in figure 5 which shows the linear variation of $M(H,T)/T^{1-\alpha}$ with H/T in the low-T and low-H region. In this context, we note that a recent theoretical work concerning the isolated Kagomé net predicts a sub-Curie local susceptibility, $\chi_{loc} \propto T^{-\alpha}$ ($\alpha < 1$), in the absence of any form of disorder [15]. This feature is the signature of a low-energy spin-liquid regime where the spin correlations have a rapid decay in space, but a slow decay in time due to a large density of triplet states. If it has a physical meaning, the power-law behaviour could also originate from a random-exchange behaviour [16] or from a quantum critical behaviour, as previously suggested for SCGO [17].

4. Conclusion

Overall, the thermodynamic properties as well as the neutron scattering features of BSGZCO resemble those of SCGO. For both systems, a paramagnetic state with short-range dynamic or quasi-static correlations extends to low temperatures in the presence of a significant amount of site dilution. A noticeable difference concerns the low-temperature behaviour of the bulk susceptibility $\chi(T)$, above the spin-glass-like transition. Further systematic studies are required to achieve a quantitative understanding of this new interesting pyrochlore slab system.

Acknowledgments

We thank P Mendels and D Bono for interesting discussions.

References

[1] See for instance Gingras M J P (ed) 2001 *Proc. Highly Frustrated Magnetism Conf. (Waterloo, 2000)*; *Can. J. Phys.* **79** 1283–1597
[2] Hagemann I S, Huang Q, Gao X P A, Ramirez A P and Cava R J 2001 *Phys. Rev. Lett.* **86** 894
[3] Obradors X, Labarta A, Isalgue A, Tejada J, Rodriguez J and Pernet M 1988 *Solid State Commun.* **65** 189
[4] Sharpf O and Capellmann H 1993 *Phys. Status Solidi* A **135** 359
[5] Rodriguez-Carvajal J 1998 *FULPROFF Version 3.5d* Laboratoire Léon Brillouin (CEA-CNRS)
[6] Limot L, Mendels P, Collin G, Mondelli C, Ouladdiaf B, Mutka H, Blanchard N and Mekata M 2002 *Phys. Rev.* B **65** 144447
[7] Martinez B, Sandiumenge F, Rouco A, Labarta A, Rodriguez-Carvajal J, Tovar M, Causa M T, Gali S and Obradors X 1992 *Phys. Rev.* B **46** 10786
[8] Mondelli C, Mutka H and Payen C 2001 *Can. J. Phys.* **79** 359
[9] Mydosh J A 1993 *Spin Glasses—An Experimental Introduction* (London: Taylor and Francis)
[10] Mondelli C, Andersen K, Mutka H, Payen C and Frick B 1999 *Physica* B **267/268** 139
[11] Lee S H, Broholm C, Ratcliff W, Gasparovic G, Huang Q, Kim T H and Cheong S W 2002 *Nature* **418** 856
[12] Mutka H, Bonnet P, Payen C, Ritter C, Danot M and Fabritchnyi P 2004 *Physica* B at press
[13] Ratcliff W II, Lee S H, Broholm C, Cheong S W and Huang Q 2002 *Phys. Rev.* B **65** 220406
[14] Schiffer P and Daruka I 1997 *Phys. Rev.* B **56** 13712
[15] Georges A, Siddharthan R and Florens S 2001 *Phys. Rev. Lett.* **87** 277203
[16] Bhatt R N and Lee P A 1982 *Phys. Rev. Lett.* **48** 344
[17] Mondelli C, Mutka H, Payen C, Frick B and Andersen K 2000 *Physica* B **284–288** 1371